



LIGO Scientific Collaboration
Virgo Collaboration

start time
15:00 UTC

Tests of General Relativity with Binary Black Holes from GWTC-2

testing GR paper

dcc.ligo.org/LIGO-P2000091/public
[arXiv:2010.14529]

data release

dcc.ligo.org/LIGO-P2000438/public

presentation slides

dcc.ligo.org/LIGO-G2002002/public

related papers

detection catalog

dcc.ligo.org/LIGO-P2000061/public
[arXiv:2010.14527]

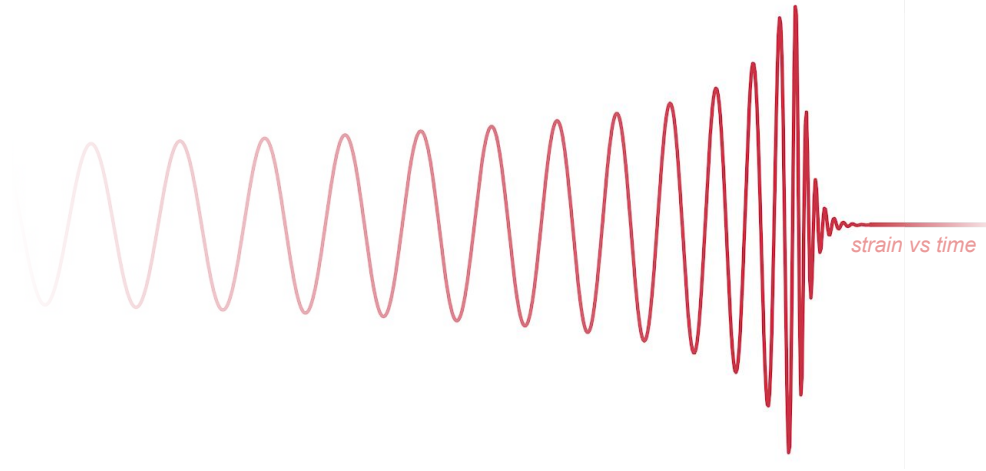
astrophysical populations

dcc.ligo.org/LIGO-P2000077/public
[arXiv:2010.14533]

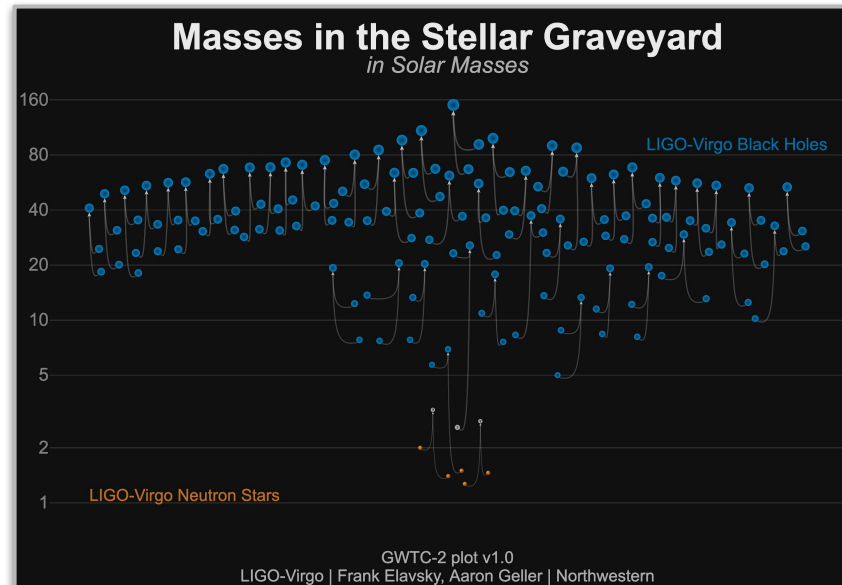


tests of GR with BBHs from GWTC-2

- 8 tests of general relativity, or modeling systematics
- 24 binary-black-hole events (FAR < 1 per 1000 yrs)
- event-by-event and collective results from sets of events



- 8 tests of general relativity, or modeling systematics
- 24 binary-black-hole events (FAR < 1 per 1000 yrs)
- event-by-event and collective results from sets of events





panelists



Sergei Ossokine

Albert Einstein Institute Potsdam

consistency tests



Geraint Pratten

University of Birmingham

source dynamics



Rico Lo

California Institute of Technology

remnant properties



Anuradha Gupta

The University of Mississippi

dispersion & polarization



Maximiliano Isi

Massachusetts Institute of Technology

moderator

consistency tests

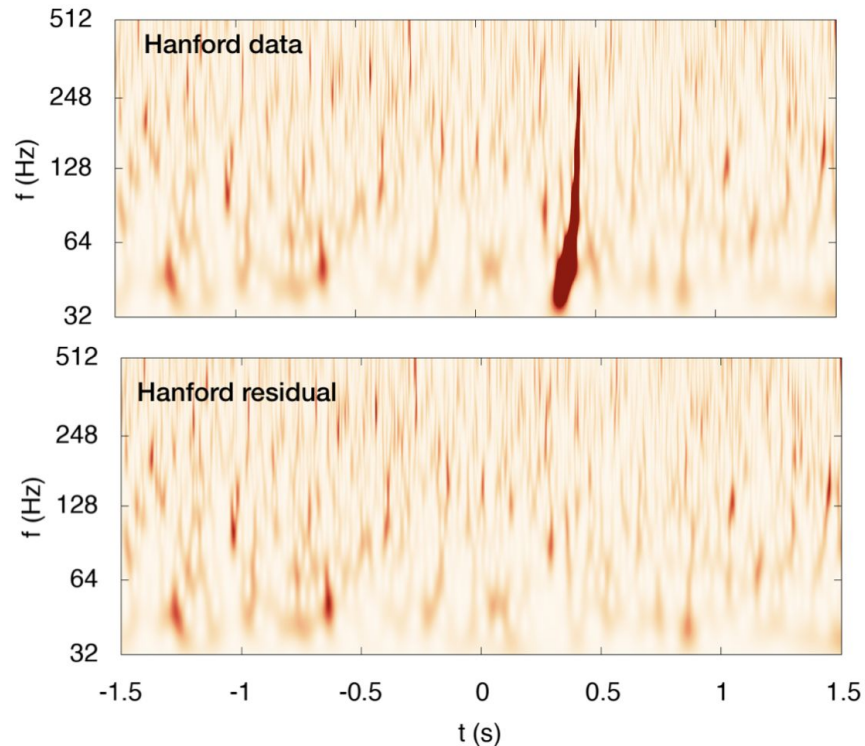
Sergei Ossokine

residuals test

- Subtract the best fit template for the event from the strain data and compute the **90% upper limit on residual SNR**.
- Check whether the residual SNR is consistent with SNR from noise: measure SNR from noise-only times around the event times, yielding a p-value

$$p = P(\text{SNR}_n \geq \text{SNR}_{\text{residual}} \mid \text{noise})$$

- If GR model is good fit to the data we expect:
 - No correlation between the SNR of the event and residual SNR
 - p-values indicating consistency with noise.

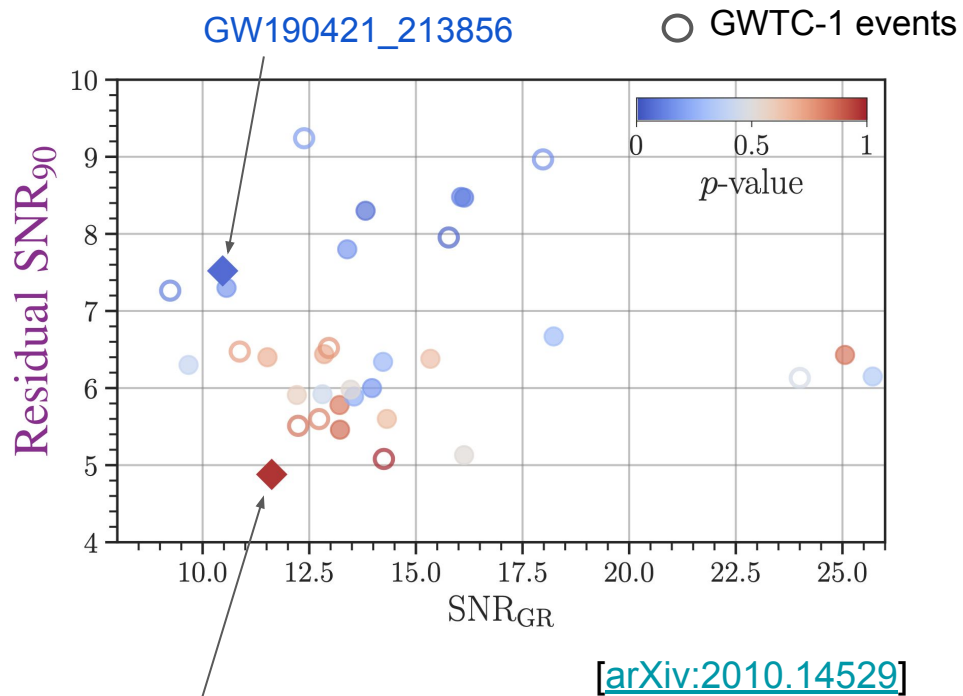


residuals test

- Subtract the best fit template for the event from the strain data and compute the **90% upper limit on residual SNR**.
- Check whether the residual SNR is consistent with SNR from noise: measure SNR from noise-only times around the event times, yielding a p-value

$$p = P(\text{SNR}_n \geq \text{SNR}_{\text{residual}} \mid \text{noise})$$

- If GR model is good fit to the data we expect:
 - No correlation between the SNR of the event and residual SNR
 - p-values indicating consistency with noise.



GW190727_060333

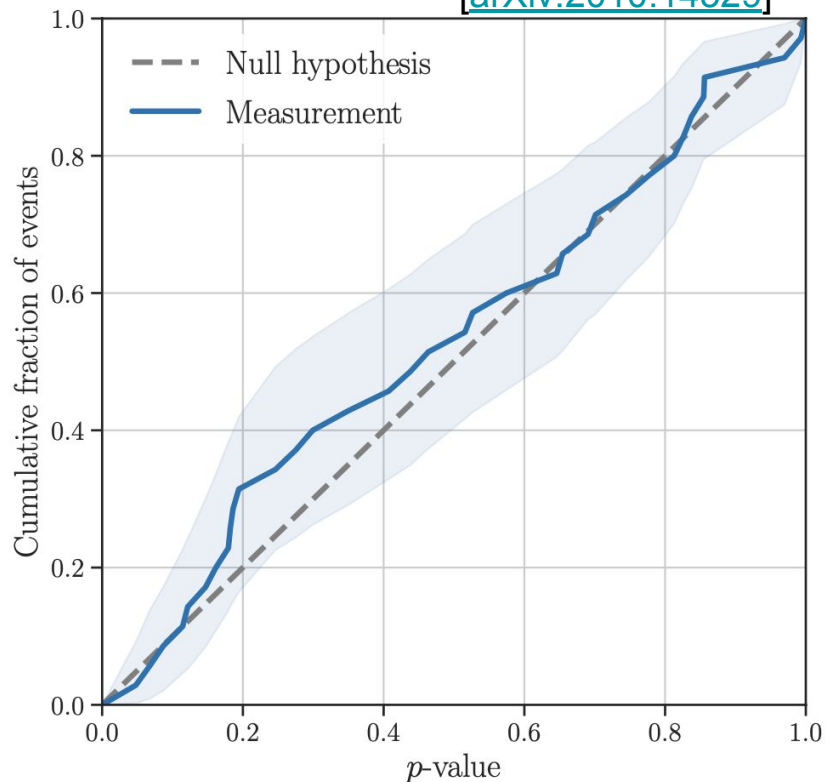


residuals test

Events	SNR _{GR}	Residual SNR ₉₀	FF ₉₀	p-value
GW190408_181802	16.06	8.48	0.88	0.15
GW190412	18.23	6.67	0.94	0.30
GW190421_213856	10.47	7.52	0.81	0.07
GW190503_185404	13.21	5.78	0.92	0.83
GW190512_180714	12.81	5.92	0.91	0.44
GW190513_205428	12.85	6.44	0.89	0.70
GW190517_055101	11.52	6.40	0.87	0.69
GW190519_153544	15.34	6.38	0.92	0.65
GW190521	14.23	6.34	0.91	0.28
GW190521_074359	25.71	6.15	0.97	0.35
GW190602_175927	13.22	5.46	0.92	0.86
GW190630_185205	16.13	5.13	0.95	0.52
GW190706_222641	13.39	7.80	0.86	0.18
GW190707_093326	13.55	5.89	0.92	0.25
GW190708_232457	13.97	6.00	0.92	0.19
GW190720_000836	10.56	7.30	0.82	0.18
GW190727_060333	11.62	4.88	0.92	0.97
GW190728_064510	13.47	5.98	0.91	0.53
GW190814	25.06	6.43	0.97	0.84
GW190828_063405	16.13	8.47	0.89	0.12
GW190828_065509	9.67	6.30	0.84	0.41
GW190910_112807	14.32	5.60	0.93	0.65
GW190915_235702	13.82	8.30	0.86	0.09
GW190924_021846	12.21	5.91	0.90	0.57

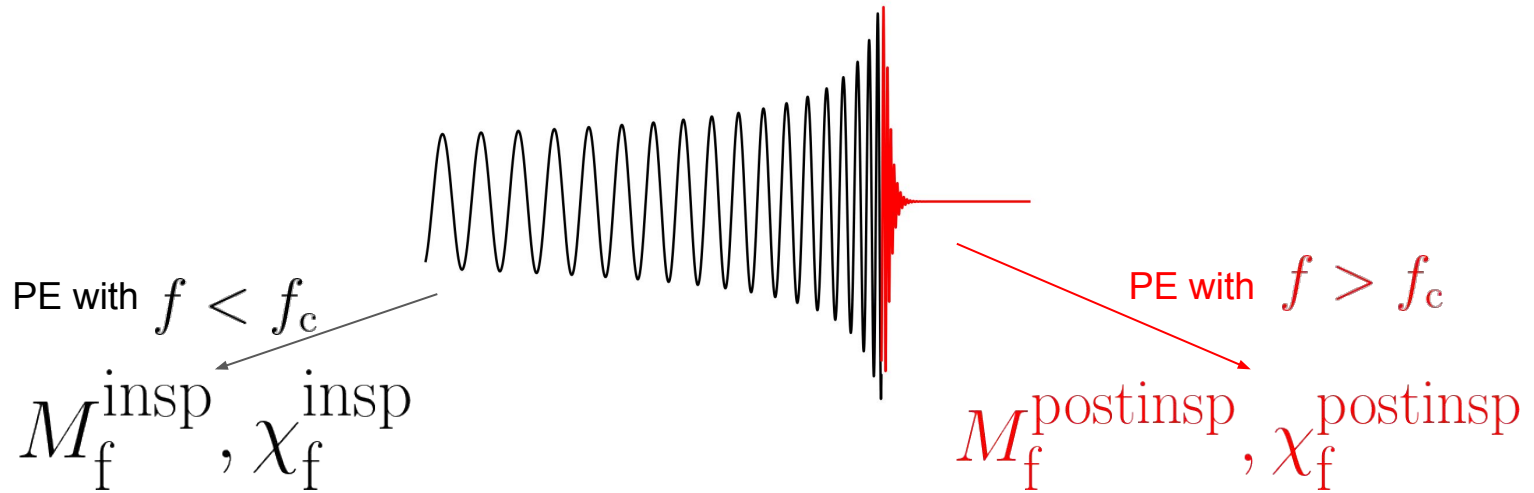
All p-values consistent with residual SNR produced by noise

[arXiv:2010.14529]



inspiral-merger-ringdown (IMR) consistency

- If GR is correct, the final state of a BBH merger is a Kerr BH.
- The final mass and spin of the BH inferred from high and low frequency regimes must be consistent.
- Use parameter estimation on full signal and NR-calibrated fits to infer the final masses and spins, and obtain the cutoff frequency f_c splitting signal into inspiral and merger-ringdown regimes.





inspiral-merger-ringdown (IMR) consistency

$$\frac{\Delta M_f}{\bar{M}_f} = 2 \frac{M_f^{\text{insp}} - M_f^{\text{postinsp}}}{M_f^{\text{insp}} + M_f^{\text{postinsp}}}$$

$$\frac{\Delta \chi_f}{\bar{\chi}_f} = 2 \frac{\chi_f^{\text{insp}} - \chi_f^{\text{postinsp}}}{\chi_f^{\text{insp}} + \chi_f^{\text{postinsp}}}$$

- For this test to be applicable, the inspiral and merger-ringdown regions of the signal must be informative.
- Impose a cut on SNR: both inspiral and merger ringdown regimes must have optimal SNR > 6.
- Additionally, demand that the detector frame total mass is below 100 solar masses.
- Reweight the posteriors to a prior uniform in deviation parameters.

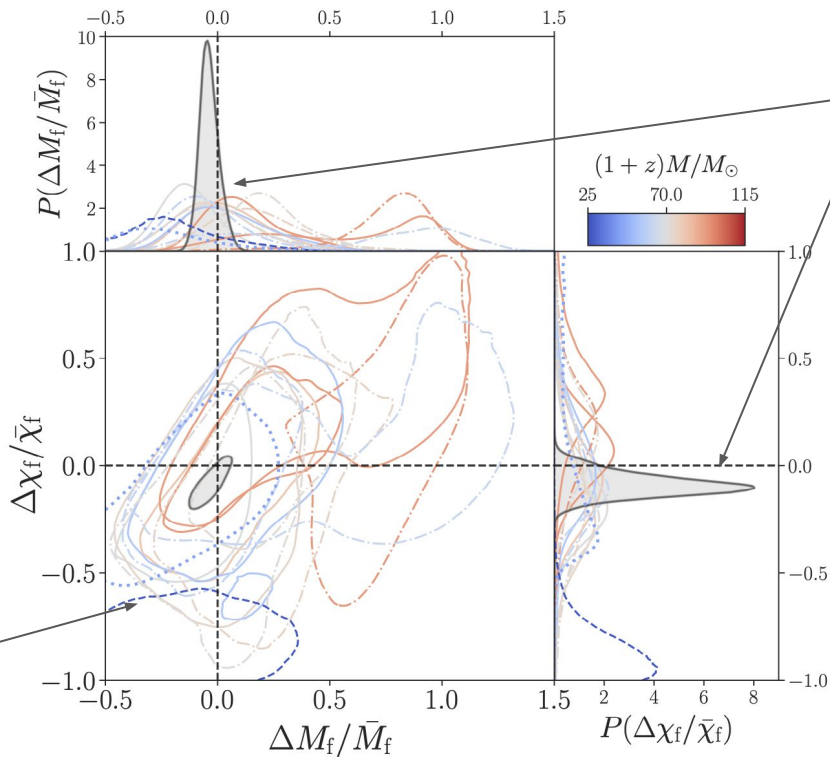


waveform systematics

- The GR waveform models we use do not exactly correspond to the true GR signal due to:
 - Approximations: theoretical underpinnings (e.g. post-Newtonian theory), modelling choices, incorporation of numerical relativity information, accuracy of NR information itself,...
 - Physical content: modes included, precession, etc.
- Any such systematics will influence tests that seek to measure deviations from GR.
- To estimate the impact of these systematic uncertainties, we usually perform analyses with multiple independent waveform models.
- Three frequently used families:
 - IMRPhenom - phenomenological PN-based models, calibrated to NR
 - SEOB - effective-one-body (EOB) models, calibrated to NR
 - NRSur - directly interpolate NR waveforms
- For the IMR consistency test, we use the precessing model IMRPhenomPv2 and the aligned-spin model SEOBNRv4_ROM, which both include the dominant quadrupolar modes only.

IMRPhenomPv2

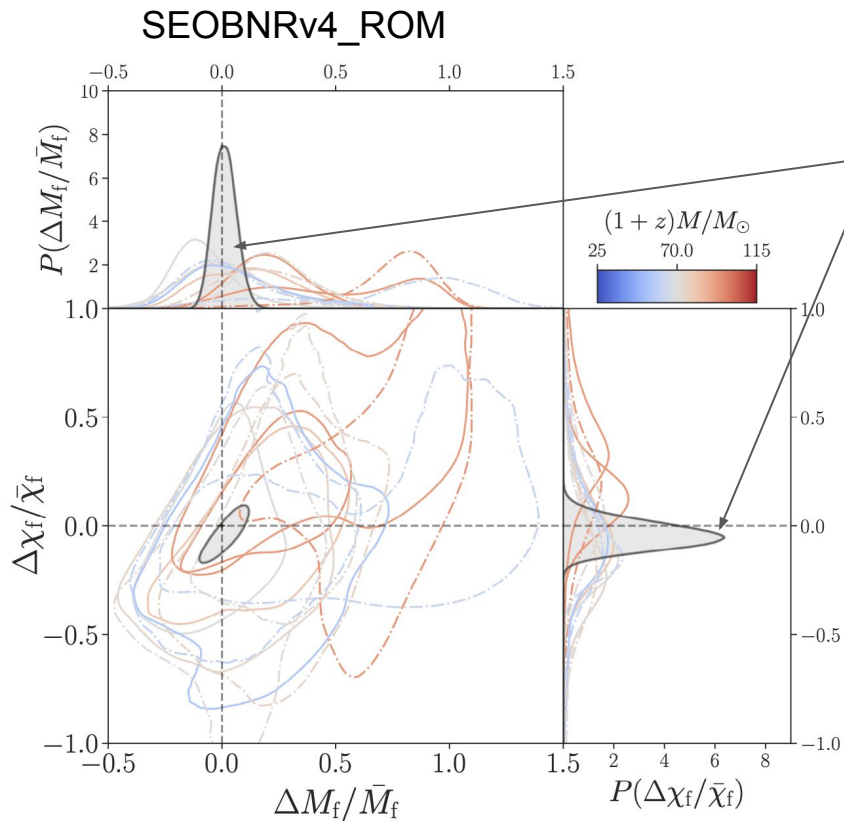
Shown are 90% credible regions



Assuming deviations are the same for all events

GW190814

Shown are 90% credible regions



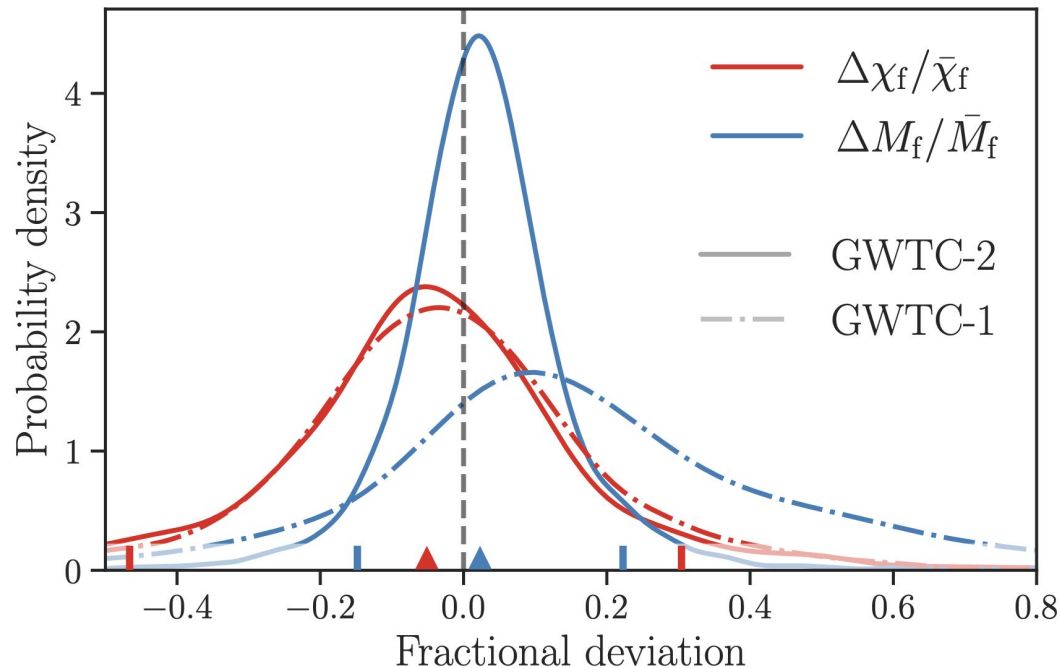
Assuming deviations are the same for all events

- Hierarchically combine results from individual events.
- Model the deviations as coming from a Gaussian distribution with unknown mean (μ) and standard deviation (σ).
- Marginalise over the population parameters:

$$p(x | d) = \int p(x | \mu, \sigma) p(\mu, \sigma | d) d\mu d\sigma$$

$$x = \left\{ \frac{\Delta M_f}{\bar{M}_f}, \frac{\Delta \chi_f}{\bar{\chi}_f} \right\}$$

Results from the population

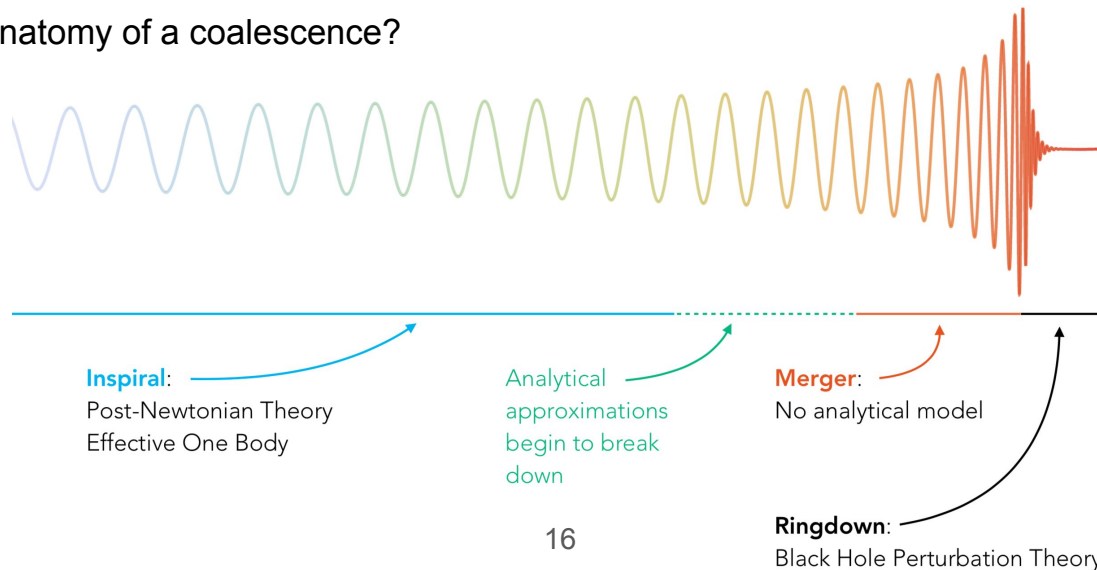


source dynamics

Geraint Pratten

parameterized Tests

- Why parameterized tests?
 - Lack of mature alternative theories: Well-posed? Physically viable? Well-defined predictions for GW signal?
 - Significant work required before widespread use of beyond-GR models in GW data analysis
- So what strategies can we adopt?
 - Quantify *generic* deviations from GR predictions → constrain degree to which deviations agree with data
- Insights from the anatomy of a coalescence?



parameterized Tests

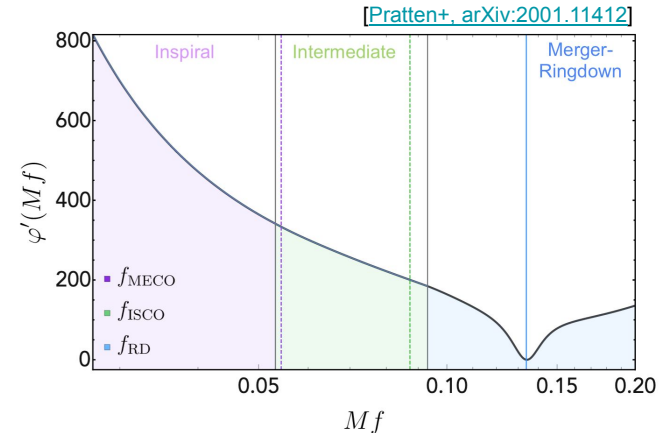
- Inspiral-Merger-Ringdown (IMR) waveform model written as frequency-dependent amplitude and phase

$$\tilde{h}(f) = \mathcal{A}(f) e^{i\varphi(f)}$$

- Parameterize phase corrections in 3 distinct regions:

- Inspiral $\varphi_{\text{Ins}}(f) = \varphi_{\text{ref}} + 2\pi f t_{\text{ref}} + \varphi_{\text{Newt}}(Mf)^{-5/3} + \varphi_{0.5\text{PN}}(Mf)^{-4/3} + \varphi_{1\text{PN}}(Mf)^{-1} + \varphi_{1.5\text{PN}}(Mf)^{-2/3} + \dots$

Coefficients analytically known in GR



- Phenomenological Coefficients

- Intermediate $\varphi_{\text{Int}} = \frac{1}{\eta} \left(\beta_0 + \beta_1 f + \beta_2 \log(f) - \frac{\beta_3}{3} f^{-3} \right)$

- Merger-Ringdown $\varphi_{\text{MR}} = \frac{1}{\eta} \left\{ \alpha_0 + \alpha_1 f - \alpha_2 f^{-1} + \frac{4}{3} \alpha_3 f^{3/4} + \alpha_4 \tan^{-1} \left(\frac{f - \alpha_5 f_{\text{RD}}}{f_{\text{damp}}} \right) \right\}$

Caution: Coefficients calibrated against NR but are not expressed in parameters relevant to GR or modified theories of gravity...

Parameterized Tests

- Constrain deviations with *parametric deformations* to GR model varying one coefficient at a time

$$p_i \rightarrow (1 + \delta\hat{p}_i)p_i \quad p_i = \{\varphi_i, \beta_i, \alpha_i\}$$

- Variant of parameterized post-Einsteinian (pPE) framework
- Use *two independent* approaches with *two different* waveform models:
 - Directly modify PN and phenomenological coefficients in *Phenom*
 - Add deformations corresponding to the inspiral coefficients to an underlying *SEOBNR* waveform
- 10 Inspiral Coefficients (*Phenom* and *SEOBNR*):

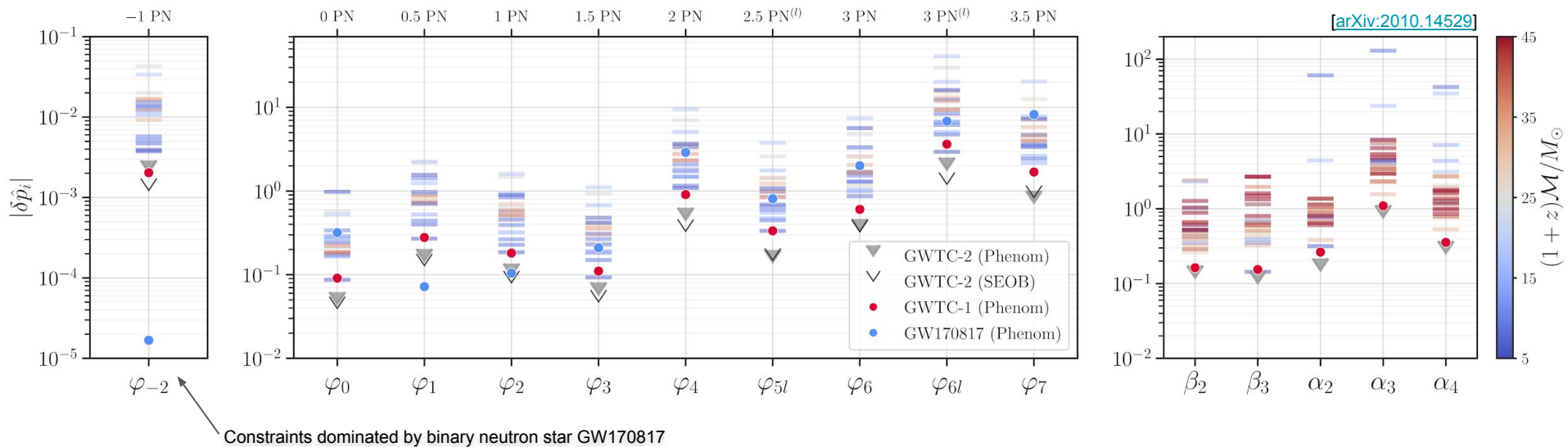
$$\{\delta\hat{\varphi}_{-2}, \delta\hat{\varphi}_0, \delta\hat{\varphi}_1, \delta\hat{\varphi}_2, \delta\hat{\varphi}_3, \delta\hat{\varphi}_4, \delta\hat{\varphi}_{5l}, \delta\hat{\varphi}_6, \delta\hat{\varphi}_{6l}, \delta\hat{\varphi}_7\} \propto f^{(i-5)/3}$$

- 5 Post-inspiral Coefficients (*Phenom*):

$$\{\beta_2, \beta_3\}, \{\alpha_2, \alpha_3, \alpha_4\}$$

parameterized Tests

- 90% upper bounds on absolute magnitude of GR violating parameters
- Lighter (*heavier*) binaries *typically* have better constraining power for *inspiral* (*post-inspiral*) coefficients
- Improvements consistent with increased sample size - broad improvement over GWTC-1

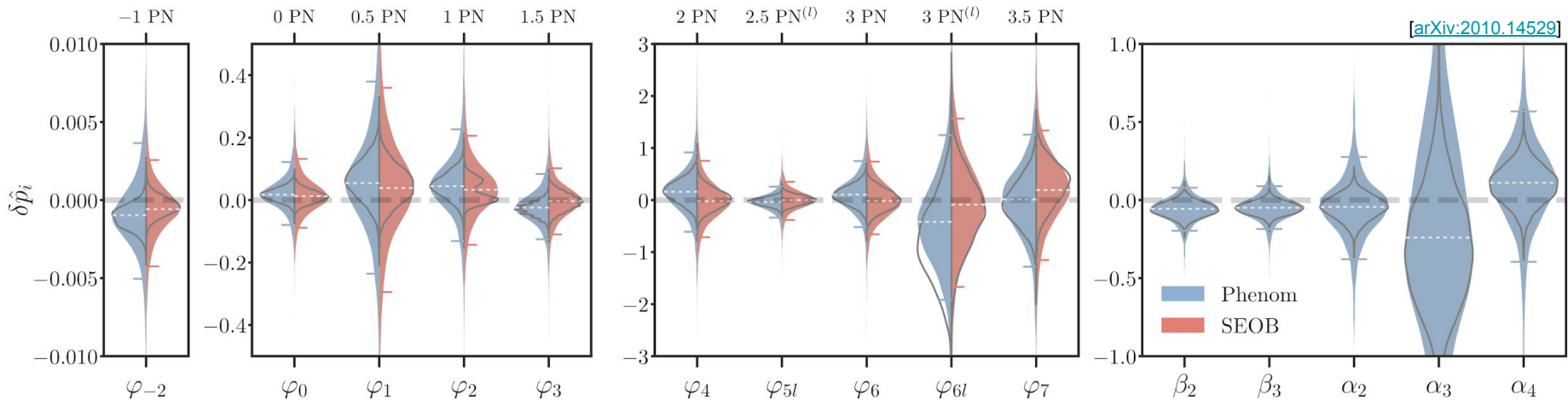


parameterized Tests

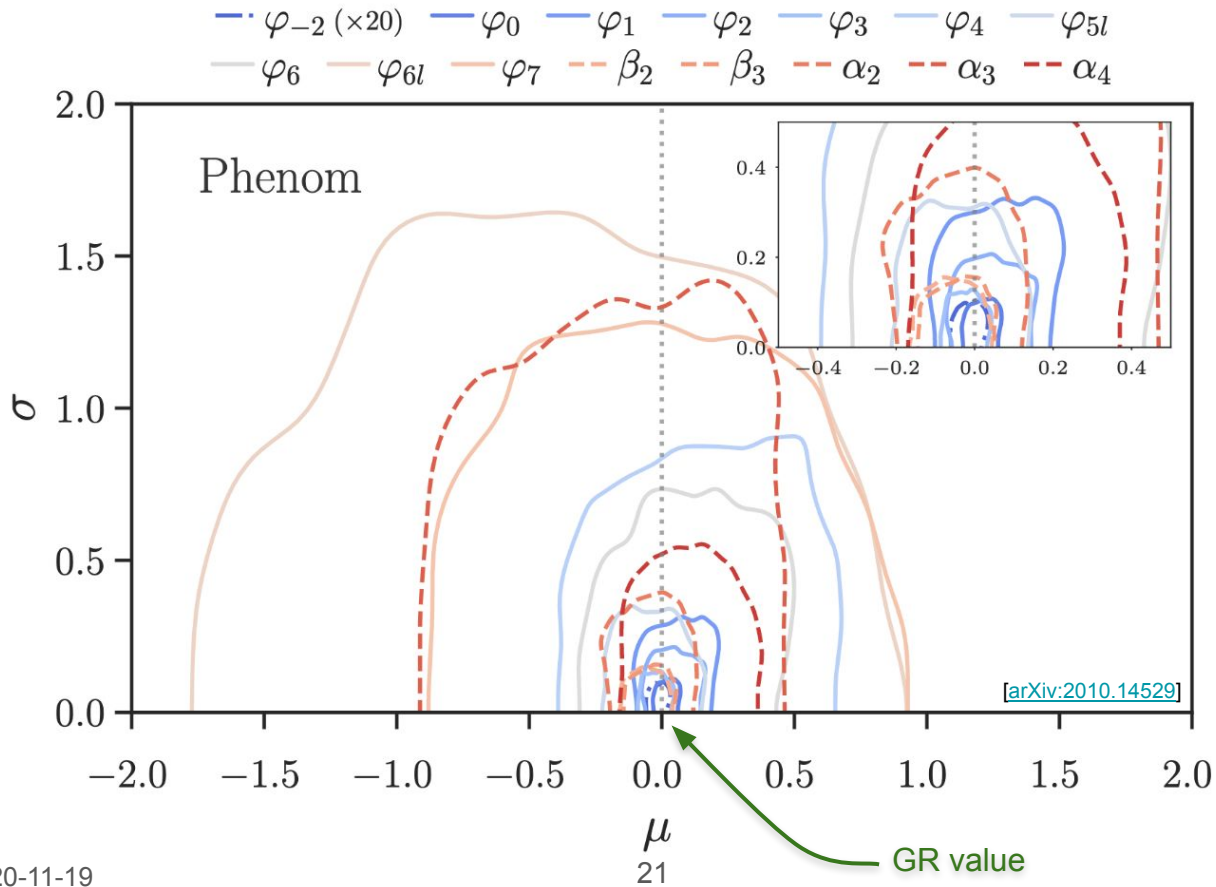
- Construct joint posteriors using two approaches:
 - Shared common value of deviation parameter
 - Hierarchical analysis
- Distributions and hyperparameters must be consistent with

GR: $\delta\hat{p}_i = 0, \mu = \sigma = 0$

- Dashed horizontal line is GR limit (vanishing deformations)
- Shaded regions: population-marginalized expectations from hierarchical analysis for *Phenom* and *SEOB*
- Black distributions: events share common value of parameter



parameterized Tests



- Hyperparameters for parameterized deviation-coefficients
- GR limit:

$$\mu = \sigma = 0$$

- Similar result for SEOB

spin-induced quadrupole moment

- Spinning motion of a compact object creates a distortion in the mass distribution
- Induces a distortion in the gravitational field measured by the quadrupole-moment tensor Q
- Effect imprinted in emitted GW radiation at specific PN orders - specialized variant of parameterized test
 - Include leading order correction at 2PN and a correction at 3PN
- For a compact object of mass m and spin χ

$$Q = -(1 + \delta\kappa) \chi_A^2 m_A^3$$



Coefficient depends on the equation of state,
mass and spin of compact object...

Enables us to test the black hole nature of the
compact object!

Black Holes (<i>no-hair conjecture</i>)	$\delta\kappa = 0$ [Poisson '98]
Neutron Stars	$\delta\kappa \sim 1 - 13$ [Laarakkers '97, Pappas '12]
Boson Stars	$\delta\kappa \sim 10 - 150$ [Ryan '97]

spin-induced quadrupole moment

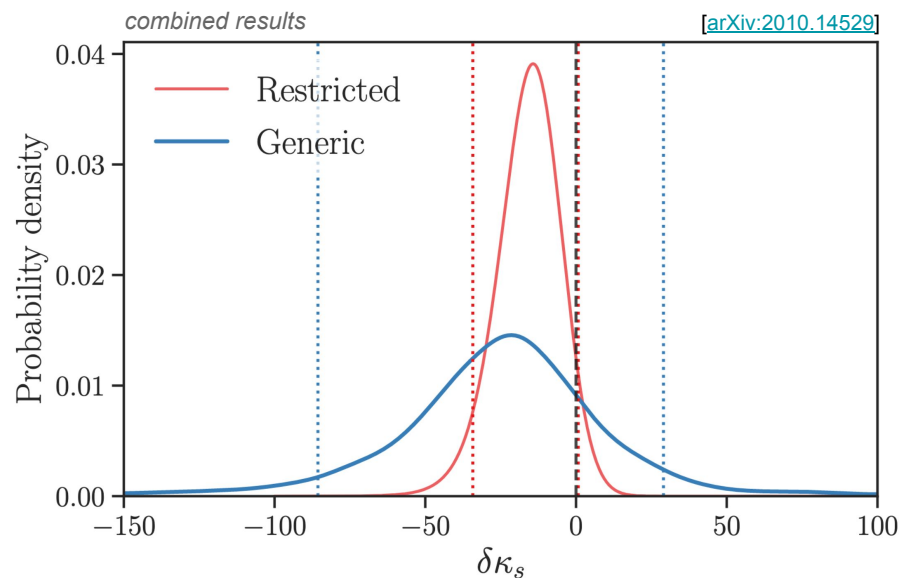
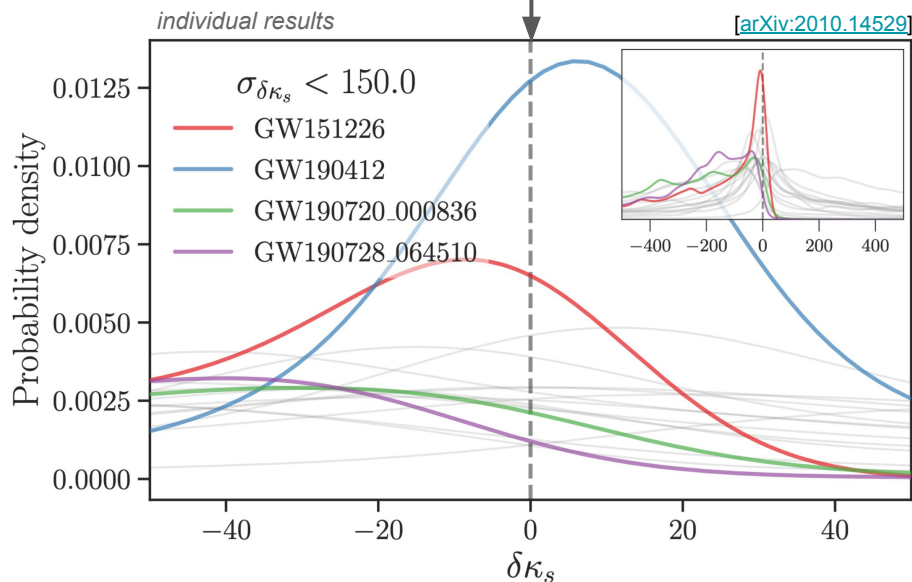
- Highly correlated with masses and spins, adopt an alternative parameterisation (cf χ_{eff})

$$\kappa_s = (\kappa_1 + \kappa_2) / 2$$

$$\kappa_a = (\kappa_1 - \kappa_2) / 2$$

For black holes the coefficients are $\kappa = 1$, so we set this term to zero

Black holes in GR have $\delta\kappa_s = 0$

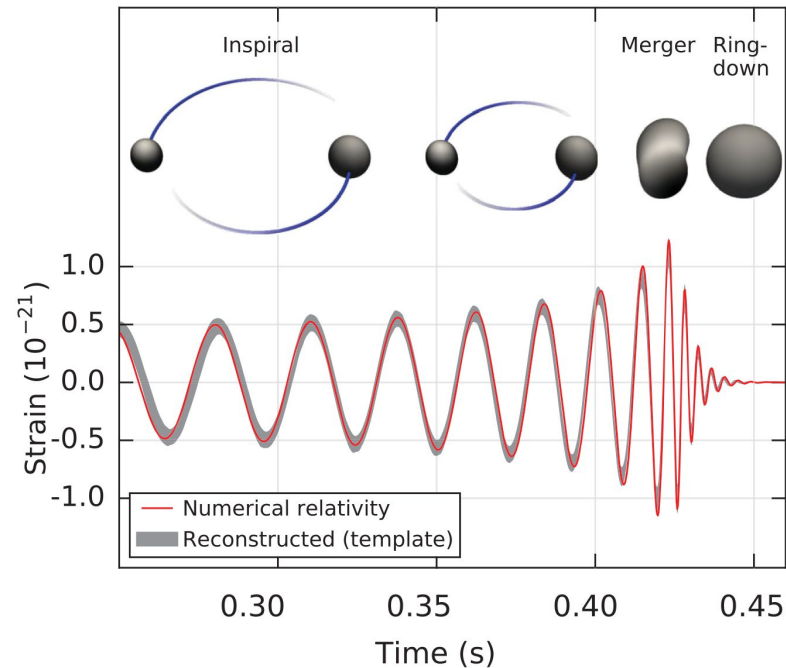


remnant properties

Rico Lo



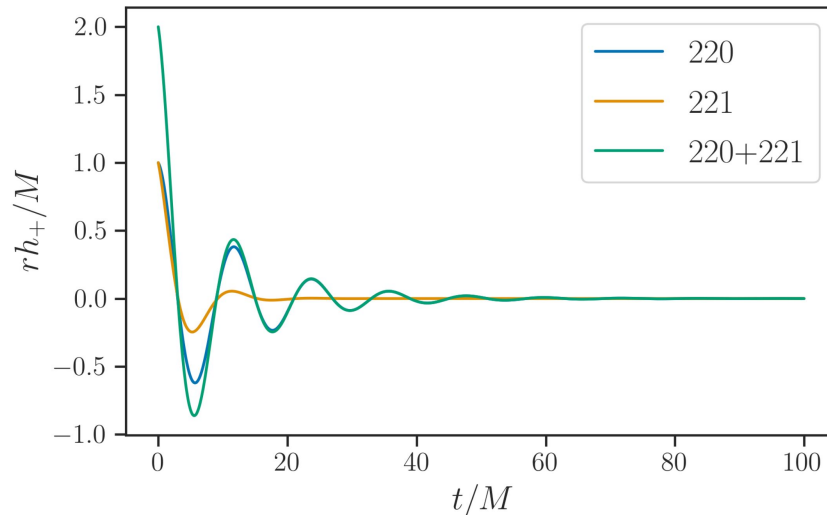
- Ringdown: quasi-normal modes (QNMs) with set frequencies and damping times
 - **Infer final mass and final spin** independent of inspiral
 - **Constrain deviations from GR** predictions of the frequencies and damping times
- Key results (qualitatively):
 - Measurements of the final mass and the spin **consistent** with the measurements using the full IMR signals
 - Inferred QNM frequencies and damping times **consistent** with BH perturbation theory calculations



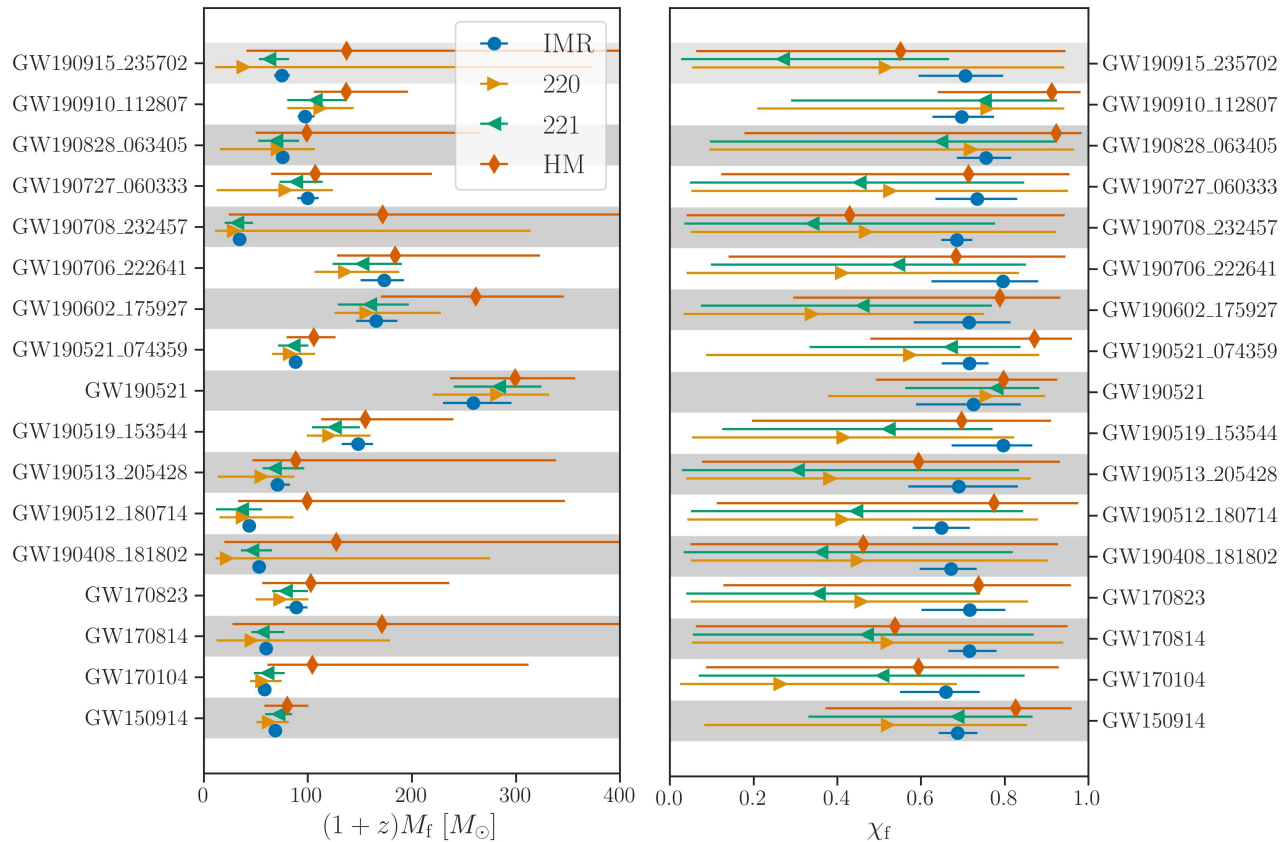
Credit: Phys. Rev. Lett. 116, 061102 (2016)

$$h_+(t) - ih_\times(t) = \sum_{\ell=2}^{+\infty} \sum_{m=-\ell}^{\ell} \sum_{n=0}^{+\infty} \mathcal{A}_{\ell mn} \exp\left[-\frac{t-t_0}{(1+z)\tau_{\ell mn}}\right] \exp\left[\frac{2\pi i f_{\ell mn}(t-t_0)}{1+z}\right] {}_{-2}S_{\ell mn}(\theta, \phi, \chi_f)$$

- Mass and spin measurement using 3 different ringdown-only waveforms
 - **Kerr₂₂₀**: include only $\ell = 2, |m| = 2, n = 0$ mode
 - **Kerr₂₂₁**: include both $\ell = 2, |m| = 2, n = 0, 1$ mode
 - **Kerr_{HM}**: include all the fundamental modes ($n = 0$) for $\ell \leq 4$



ringdown





ringdown

No significant evidence for HM in ringdown

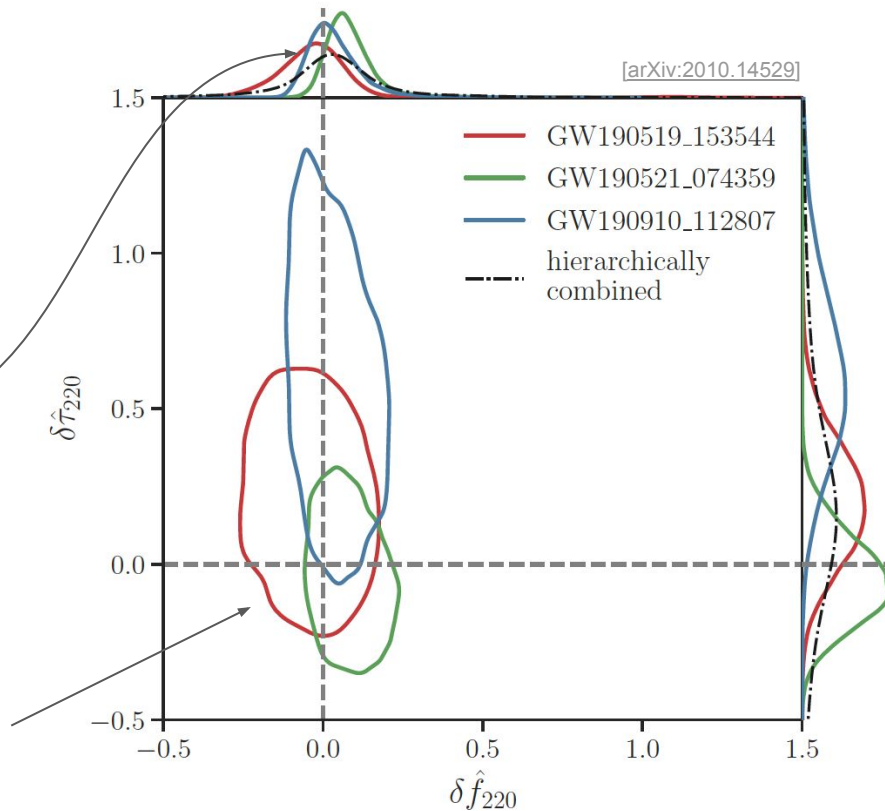
Event	Redshifted final mass (1+z) M_f [M_\odot]				Final spin χ_f				Higher modes	Overtones	
	IMR	Kerr ₂₂₀	Kerr ₂₂₁	Kerr _{HM}	IMR	Kerr ₂₂₀	Kerr ₂₂₁	Kerr _{HM}	$\log_{10} \mathcal{B}_{220}^{\text{HM}}$	$\log_{10} \mathcal{B}_{220}^{221}$	$\log_{10} \mathcal{O}_{\text{GR}}^{\text{modGR}}$
GW150914	68.8 ^{+3.6} _{-3.1}	62.7 ^{+19.0} _{-12.1}	71.7 ^{+13.2} _{-12.5}	80.3 ^{+20.1} _{-21.7}	0.69 ^{+0.05} _{-0.04}	0.52 ^{+0.33} _{-0.44}	0.69 ^{+0.18} _{-0.36}	0.83 ^{+0.13} _{-0.45}	0.03	0.63	-0.34
GW170104	58.5 ^{+4.6} _{-4.1}	56.2 ^{+19.1} _{-11.6}	61.3 ^{+16.7} _{-13.2}	104.3 ^{+207.7} _{-43.1}	0.66 ^{+0.08} _{-0.11}	0.26 ^{+0.42} _{-0.24}	0.51 ^{+0.34} _{-0.44}	0.59 ^{+0.34} _{-0.51}	0.26	-0.20	-0.23
GW170814	59.7 ^{+3.0} _{-2.3}	46.1 ^{+133.0} _{-33.6}	56.6 ^{+20.9} _{-11.1}	171.2 ^{+268.7} _{-143.5}	0.72 ^{+0.07} _{-0.05}	0.52 ^{+0.42} _{-0.47}	0.47 ^{+0.40} _{-0.42}	0.54 ^{+0.41} _{-0.48}	0.04	-0.19	-0.11
GW170823	88.8 ^{+11.2} _{-10.2}	73.8 ^{+26.8} _{-23.7}	79.0 ^{+21.3} _{-13.2}	103.0 ^{+133.1} _{-46.7}	0.72 ^{+0.09} _{-0.12}	0.46 ^{+0.40} _{-0.41}	0.36 ^{+0.38} _{-0.32}	0.74 ^{+0.22} _{-0.61}	0.02	-0.98	-0.07
GW190408_181802	53.1 ^{+3.2} _{-3.4}	22.4 ^{+253.0} _{-11.1}	46.6 ^{+18.8} _{-10.9}	127.4 ^{+327.7} _{-107.6}	0.67 ^{+0.06} _{-0.07}	0.45 ^{+0.45} _{-0.40}	0.36 ^{+0.46} _{-0.33}	0.46 ^{+0.47} _{-0.41}	-0.05	-1.02	-0.02
GW190512_180714	43.4 ^{+4.1} _{-2.8}	37.6 ^{+48.9} _{-22.4}	36.7 ^{+19.3} _{-24.8}	99.4 ^{+247.6} _{-66.5}	0.65 ^{+0.07} _{-0.07}	0.41 ^{+0.47} _{-0.37}	0.45 ^{+0.40} _{-0.39}	0.77 ^{+0.20} _{-0.66}	0.09	-0.42	0.03
GW190513_205428	70.8 ^{+12.2} _{-6.9}	55.5 ^{+31.5} _{-42.1}	68.5 ^{+28.2} _{-11.8}	88.7 ^{+250.0} _{-41.9}	0.69 ^{+0.14} _{-0.12}	0.38 ^{+0.48} _{-0.34}	0.31 ^{+0.53} _{-0.28}	0.59 ^{+0.34} _{-0.52}	0.09	-0.54	-0.05
GW190519_153544	148.2 ^{+14.5} _{-15.5}	120.7 ^{+39.7} _{-21.5}	125.9 ^{+24.3} _{-21.7}	155.4 ^{+84.4} _{-42.5}	0.80 ^{+0.07} _{-0.12}	0.42 ^{+0.41} _{-0.36}	0.52 ^{+0.25} _{-0.40}	0.70 ^{+0.21} _{-0.50}	0.21	-0.00	-0.11
GW190521	259.2 ^{+36.6} _{-29.0}	282.2 ^{+50.0} _{-61.9}	284.0 ^{+40.4} _{-43.9}	299.3 ^{+57.7} _{-62.4}	0.73 ^{+0.11} _{-0.14}	0.76 ^{+0.14} _{-0.38}	0.78 ^{+0.10} _{-0.22}	0.80 ^{+0.13} _{-0.30}	0.12	-0.86	-0.50
GW190521_074359	88.1 ^{+4.3} _{-4.9}	83.0 ^{+24.0} _{-17.2}	86.4 ^{+14.1} _{-14.8}	105.9 ^{+20.8} _{-26.4}	0.72 ^{+0.05} _{-0.07}	0.57 ^{+0.31} _{-0.49}	0.67 ^{+0.17} _{-0.34}	0.87 ^{+0.09} _{-0.39}	-0.04	1.29	-0.27
GW190602_175927	165.6 ^{+20.5} _{-19.2}	156.4 ^{+71.4} _{-30.6}	160.0 ^{+37.4} _{-31.2}	261.7 ^{+84.4} _{-91.5}	0.71 ^{+0.10} _{-0.13}	0.34 ^{+0.41} _{-0.31}	0.46 ^{+0.31} _{-0.39}	0.79 ^{+0.14} _{-0.49}	0.61	-1.56	0.32
GW190706_222641	173.6 ^{+18.8} _{-22.9}	136.0 ^{+52.0} _{-29.3}	152.5 ^{+37.8} _{-28.4}	184.0 ^{+139.2} _{-55.8}	0.80 ^{+0.08} _{-0.17}	0.41 ^{+0.42} _{-0.37}	0.55 ^{+0.31} _{-0.45}	0.68 ^{+0.26} _{-0.54}	-0.06	-0.64	-0.45
GW190708_232457	34.4 ^{+2.7} _{-0.7}	28.9 ^{+285.4} _{-17.9}	32.3 ^{+15.0} _{-12.2}	171.9 ^{+307.6} _{-147.8}	0.69 ^{+0.04} _{-0.04}	0.47 ^{+0.45} _{-0.42}	0.34 ^{+0.44} _{-0.31}	0.43 ^{+0.51} _{-0.39}	-0.11	-0.17	-0.02
GW190727_060333	100.0 ^{+10.5} _{-10.0}	78.7 ^{+45.7} _{-66.4}	88.8 ^{+25.7} _{-16.0}	107.4 ^{+112.1} _{-42.7}	0.73 ^{+0.10} _{-0.10}	0.53 ^{+0.42} _{-0.47}	0.45 ^{+0.39} _{-0.41}	0.71 ^{+0.24} _{-0.59}	-0.02	-1.65	-0.40
GW190828_063405	75.9 ^{+6.0} _{-5.2}	71.2 ^{+35.8} _{-55.5}	69.6 ^{+22.0} _{-17.3}	99.0 ^{+166.0} _{-49.1}	0.76 ^{+0.06} _{-0.07}	0.72 ^{+0.25} _{-0.62}	0.65 ^{+0.27} _{-0.55}	0.92 ^{+0.06} _{-0.74}	0.05	-0.72	-0.05
GW190910_112807	97.3 ^{+9.4} _{-7.1}	112.2 ^{+32.0} _{-31.7}	107.7 ^{+28.6} _{-27.4}	137.1 ^{+59.5} _{-31.4}	0.70 ^{+0.08} _{-0.07}	0.76 ^{+0.18} _{-0.55}	0.75 ^{+0.17} _{-0.46}	0.91 ^{+0.07} _{-0.27}	-0.10	-0.64	-0.40
GW190915_235702	75.0 ^{+7.7} _{-7.3}	38.3 ^{+335.1} _{-27.4}	63.0 ^{+19.1} _{-9.9}	137.3 ^{+324.1} _{-96.2}	0.71 ^{+0.09} _{-0.11}	0.52 ^{+0.43} _{-0.46}	0.27 ^{+0.40} _{-0.24}	0.55 ^{+0.39} _{-0.49}	0.06	-0.37	-0.04

Mass and spin of the final BH inferred from the inspiral part of the signal

$$\delta \hat{f}_{220} = 0.03^{+0.38}_{-0.35}$$

constrained using hierarchical analysis with a set of BBHs

contour for 90% credible region



220 mode, i.e.
 $(\ell = 2, |m| = 2, n = 0)$
 Fundamental mode

$$f_{220} = f_{220}^{\text{GR}}(1 + \delta \hat{f}_{220})$$

$$\tau_{220} = \tau_{220}^{\text{GR}}(1 + \delta \hat{\tau}_{220})$$

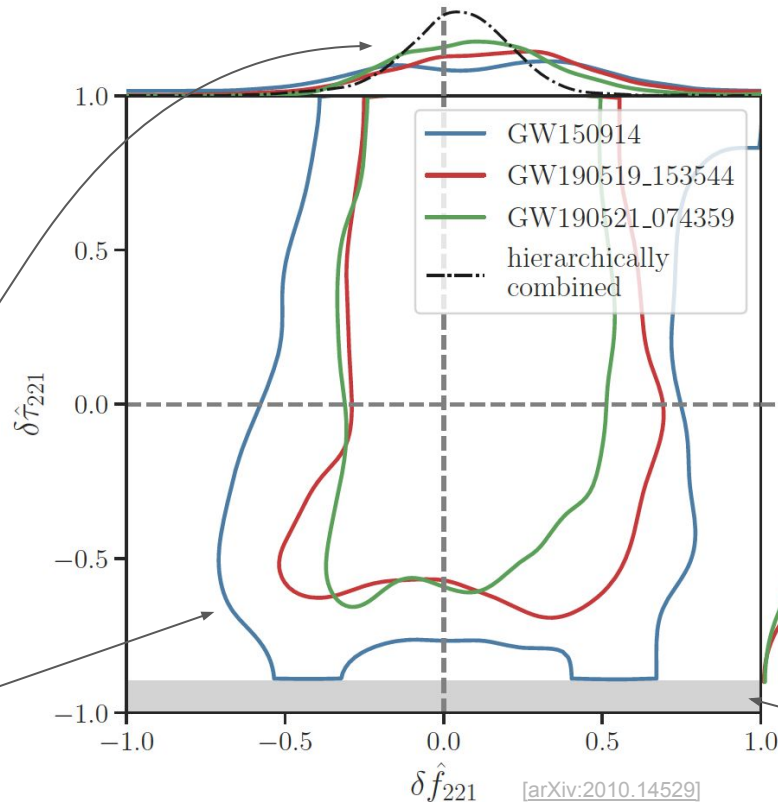
$\delta \hat{\tau}_{220} = 0.16^{+0.98}_{-0.98}$
 with a wider uncertainty

Mass and spin of the final BH inferred from the fundamental mode

$$\delta \hat{f}_{221} = 0.04^{+0.27}_{-0.32}$$

constrained using hierarchical analysis with a set of BBHs

contour for 90% credible region



221 mode, i.e.
 $(\ell = 2, |m| = 2, n = 1)$

First overtone

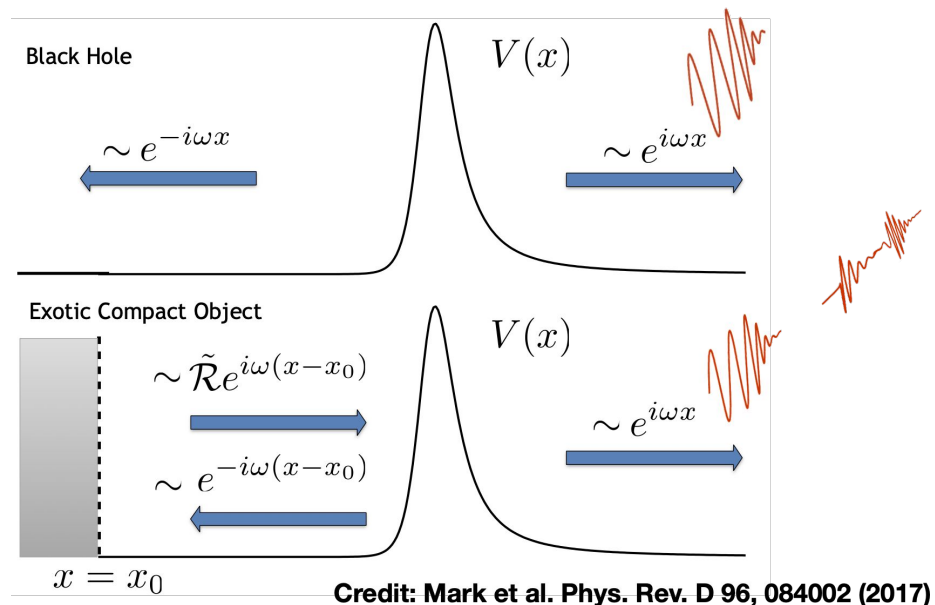
$$f_{221} = f_{221}^{\text{GR}}(M_f, \chi_f)(1 + \delta \hat{f}_{221})$$

$$\tau_{221} = \tau_{221}^{\text{GR}}(M_f, \chi_f)(1 + \delta \hat{\tau}_{221})$$

$\delta \hat{\tau}_{221}$
 virtually unconstrained

excluded by prior

- What if the remnant compact object is **not** a classical BH?
- **Exotic compact objects (ECOs)**: event horizon replaced by a reflective surface
- GWs reflecting back and forth between the surface and the light ring \Rightarrow **GW echoes**
- Inspiral + Merger + Ringdown + Echoes (IMRE)
- Smoking-gun evidence for a BH mimicker if detected





echoes

- Analyzed 31 BBHs from GWTC-2 (O1+O2+O3a) passing the FAR threshold
- Positive log Bayes factor: the IMRE model is preferred over the IMR model by the observed data, vice versa
- No significant evidence of GW echoes found**
- Most 'significant' event: GW190915_235702, the log Bayes factor is *merely 0.17*
- Not shown in the table (not passing the selection threshold): for GW151012 in O1 and for GW170729 in O2, both have negative log Bayes factor

Event	$\log_{10} \mathcal{B}_{\text{IMR}}^{\text{IMRE}}$	Event	$\log_{10} \mathcal{B}_{\text{IMR}}^{\text{IMRE}}$
GW150914	-0.57	GW170809	-0.22
GW151226	-0.08	GW170814	-0.49
GW170104	-0.53	GW170818	-0.62
GW170608	-0.44	GW170823	-0.34
GW190408_181802	-0.93	GW190706_222641	-0.10
GW190412	-1.30	GW190707_093326	0.08
GW190421_213856	-0.11	GW190708_232457	-0.87
GW190503_185404	-0.36	GW190720_000836	-0.45
GW190512_180714	-0.56	GW190727_060333	0.01
GW190513_205428	-0.03	GW190728_064510	0.01
GW190517_055101	0.16	GW190828_063405	0.10
GW190519_153544	-0.10	GW190828_065509	-0.01
GW190521	-1.82	GW190910_112807	-0.22
GW190521_074359	-0.72	GW190915_235702	0.17
GW190602_175927	0.13	GW190924_021846	-0.03
GW190630_185205	0.08		

dispersion & polarizations

Anuradha Gupta

dispersion

Generalized Dispersion Relation:

$$E^2 = p^2 c^2 + A_\alpha p^\alpha c^\alpha$$

E = Energy

p = momentum

c = speed of light

A_α, α = phenomenological parameters

GR

$A_\alpha = 0$, for all α

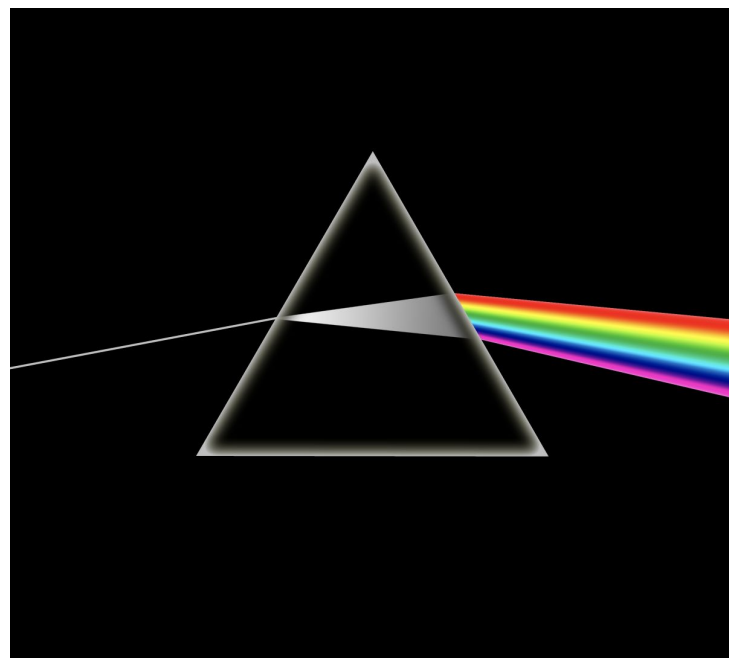
$$m_g = 0$$

Extensions of GR

Massive gravity theory:

$$\alpha = 0, A_\alpha > 0, m_g = A_0^{1/2} c^{-2}$$

$$m_g = \text{graviton mass}$$



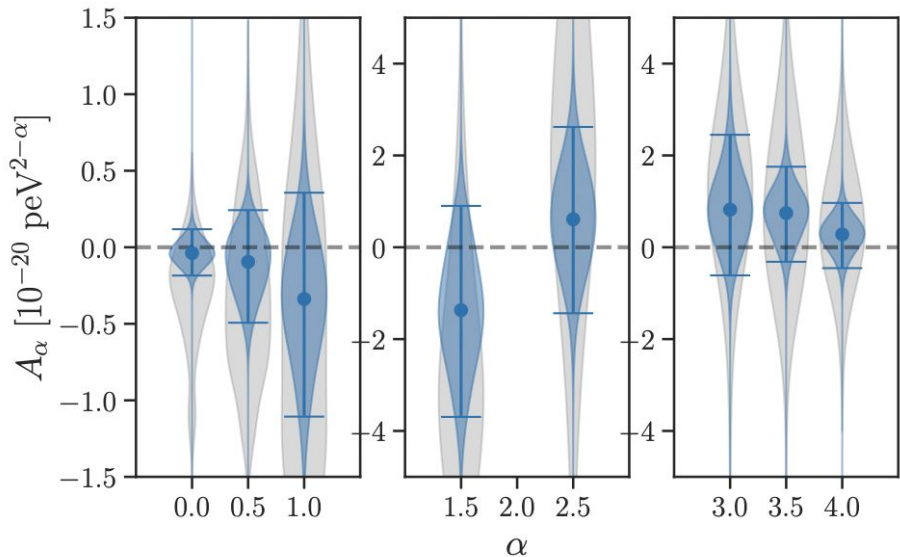
Dispersion of light wave



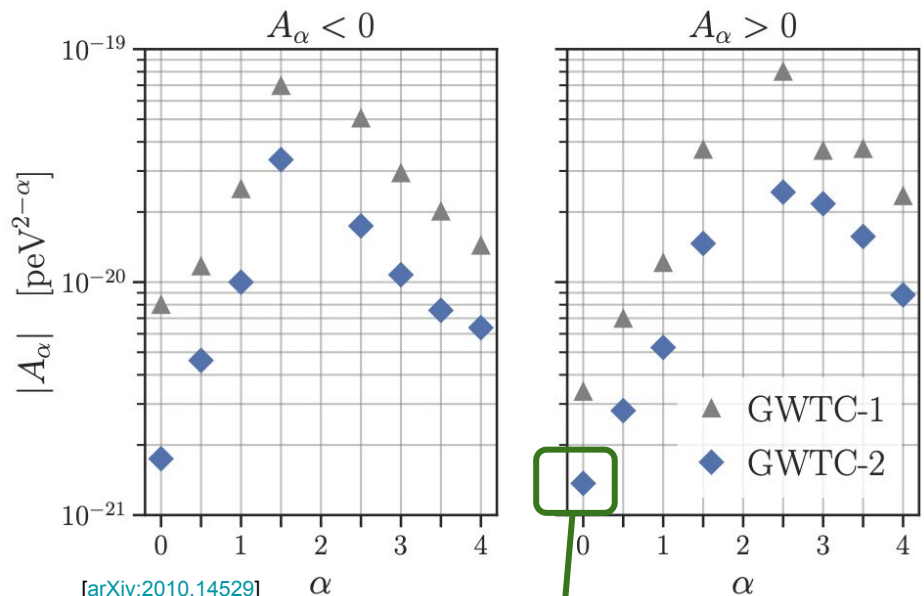
dispersion

$$\alpha = 0, 0.5, 1.0, 1.5, 2.5, 3, 3.5, 4.0$$
$$A_\alpha < 0, A_\alpha > 0$$

- Assume that the signal close to the source is given by GR, all modifications come from propagation
- Leads to the dephasing of the entire GW signal, proportional to A_α and roughly to the distance
- A_α and m_g are analysis parameters
 - flat prior in A_α
 - flat prior in m_g
- Since A_α and m_g have same values for all events, posteriors from individual events are multiplied to obtain the combined results



[\[arXiv:2010.14529\]](https://arxiv.org/abs/2010.14529)



[\[arXiv:2010.14529\]](https://arxiv.org/abs/2010.14529)

gives graviton mass

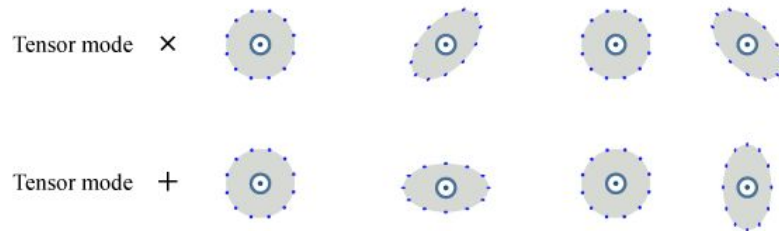


dispersion

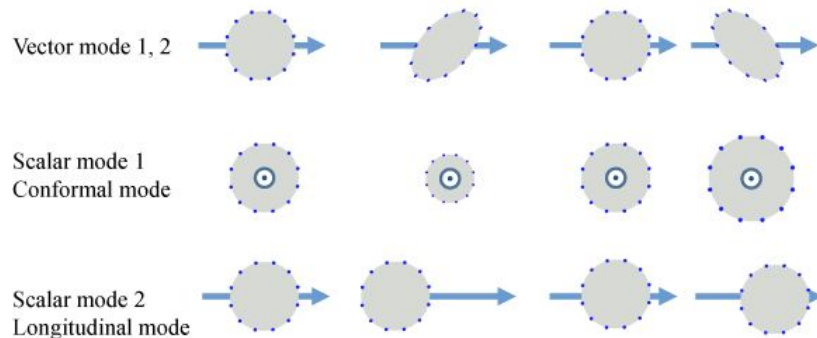
- Noticeable improvement in the upper bound of $|A_\alpha|$ as compared to GWTC-1
- A factor of ~ 2.6 improvement, consistent with the increase in number of events from GWTC-1 to GWTC-2
- $m_g \leq 1.76 \times 10^{-23} \text{ eV}/c^2$, with 90% credibility
- A factor of ~ 2.7 improvement as compared to GWTC-1
- 1.8 times more stringent than the recent Solar System bound of $3.16 \times 10^{-23} \text{ eV}/c^2$ with 90% credibility [[Phys. Rev. D 102, 021501 \(2020\)](#)]

- Generic metric theories of gravity allow up to *six* GW polarizations
 - two tensor modes (helicity ± 2), allowed in GR
 - two vector modes (helicity ± 1)
 - two scalar modes (helicity 0)
- Polarization content is imprinted in the relative amplitudes of the output at different detectors
- Used to reconstruct the GW polarization content in the data
- Five-detector network would be ideal for this test
- We used three-detector network to distinguish between specific subsets of all the possible polarization combinations

Polarizations present in GR: Fully transverse to the line of propagation



Additional Polarizations not present in GR



Credit: Claudia de Rham, LRR, 17 (2014).



polarizations

- Extreme polarization hypotheses:
 - full-tensor vs full-vector
 - full-tensor vs full-scalar
- Null-stream based polarization test, does not rely on specific waveform models
 - *Null-stream*: linear combination of data streams from different detectors
 - Free of true GW signal with a given helicity and sky-location
 - Marginalized over sky-location
 - Any excess power in the *null stream* must be produced by a different helicity and sky-location
 - Quantify the excess power by *null energy*

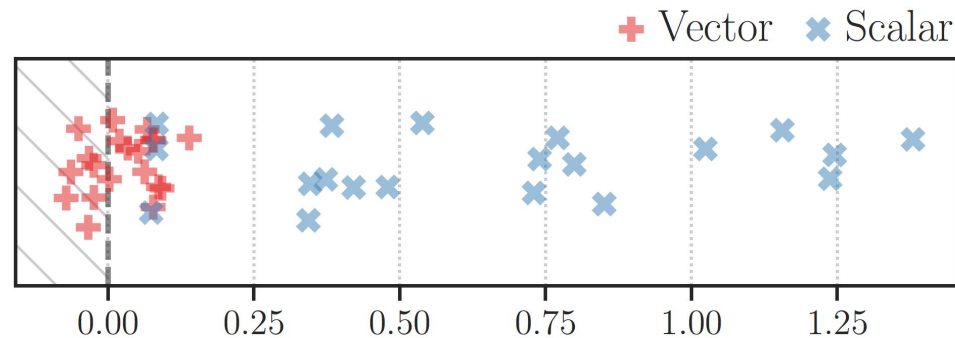
Event	$\log_{10} \mathcal{B}_V^T$	$\log_{10} \mathcal{B}_S^T$
GW170809	0.078	0.421
GW170814	-0.032	0.740
GW170818	0.002	0.344
GW190408_181802	0.076	0.480
GW190412	0.079	0.539
<u>GW190503_185404</u>	-0.072	1.245
GW190512_180714	-0.024	0.346
<u>GW190513_205428</u>	0.139	1.380
GW190517_055101	0.008	0.730
GW190519_153544	0.067	0.799
GW190521	0.093	1.156
GW190602_175927	-0.064	0.373
GW190706_222641	0.052	0.771
<u>GW190720_000836</u>	0.034	0.074
GW190727_060333	0.087	1.024
GW190728_064510	-0.024	0.083
GW190828_063405	0.063	0.851
GW190828_065509	-0.034	0.084
GW190915_235702	0.020	1.238
GW190924_021846	-0.051	0.384

\mathcal{B}_V^T = Bayes factor for full-tensor vs full-vector hypotheses

\mathcal{B}_S^T = Bayes factor for full-tensor vs full-scalar hypotheses

highest Bayes factor

lowest Bayes factors



$\log_{10} \mathcal{B}_{V/S}^T$ (tensor vs non-tensor)

[arXiv:2010.14529]

conclusion

Max Isi

- no statistically significant deviations from GR, or unaccounted systematics
- improved GWTC–1 constraints by factors of $\sim 2\text{--}3$
- introduced new analyses, and statistical techniques

more to come!

